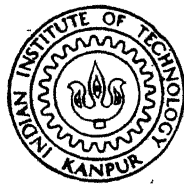


# ELECTRICAL CONDUCTIVITY OF HYDROGENATED AMORPHOUS GERMANIUM

By

ARUNA RAJVANSHI

PHY TH  
1980 PHY/1980/M  
M R 131 e  
RAJ  
EE



DEPARTMENT OF PHYSICS

INDIAN INSTITUTE OF TECHNOLOGY KANPUR  
AUGUST, 1980

# ELECTRICAL CONDUCTIVITY OF HYDROGENATED AMORPHOUS GERMANIUM

A Thesis Submitted  
in Partial Fulfilment of the Requirements  
for the Degree of  
MASTER OF PHILOSOPHY

By  
ARUNA RAJVANSHI

*to the*

**DEPARTMENT OF PHYSICS**  
**INDIAN INSTITUTE OF TECHNOLOGY KANPUR**  
**AUGUST, 1980**

I.I.T. KANPUR  
CENTRAL LIBRARY  
Acc. No. A 66963  
7 SEP 1981

PHY-1980-M-RAJ-ELE

Certificate

This is to certify that the thesis entitled "Electrical conductivity of Hydrogenated Amorphous Germanium", by ARUNA RAJVANSHI is the work carried out under my supervision and has not been submitted elsewhere for a degree.

August 7, 1980.

S.C. Agarwal  
(S.C. Agarwal)  
Department of Physics  
Indian Institute of Technology  
KANPUR - 208016.

### ACKNOWLEDGEMENT

I wish to acknowledge with deep sense of gratitude my obligations to Dr S C Agarwal for his able guidance, constant help and liberality for the successful compilation of this work.

I am greatly indebted to Miss R.V. Singh and Dr Kamala D. Edward Ex Principal and Principal, I.T. College, Lucknow respectively for taking interest in my academic improvement and being extremely understanding and helpful. The interest in my academic progress and encouragement from Dr V.K. Deshpande of Indian Institute of Technology Kanpur and also from my colleague Dr R.N. Singh of Lucknow University is gratefully acknowledged.

I take pleasure in thanking Mr Shailendra Kumar for his invaluable co-operation, kind help and assistance throughout the work. I also thank Dr P.N. Dixit and Mr D.S. Mishra for the constant encouragement and many helpful suggestions. Many thanks are due to all my friends for helping me in various ways especially Mr Mahendra Pal, Mr Atul Sen and Mr Virendra Kumar by whose efforts I could get the manuscript in this form.

I wish to thank Mr J.P. Gupta for excellent typing, Mr B.P. Jain for tracing the figures and Mr H.K. Panda for cyclostyling the thesis. Also, my thanks are to Mr Beni Prasad, the Lab. Assistant.

Financial assistance from the University Grants Commission under the Faculty Improvement Programme and from Department of Science and Technology, New Delhi is also gratefully acknowledged.

## CONTENTS

<u>Chapter</u>		<u>Page</u>
	LIST OF TABLES	i
	LIST OF FIGURES	ii
	ABSTRACT	iii
I.	INTRODUCTION	1
II.	SAMPLE PREPARATION	6
	2.1    Introduction	6
	2.2    Substrate cleaning procedure	6
	2.3    Electrode deposition	6
	2.4    Deposition of Amorphous-Germanium	7
	2.5    Deposition of hydrogenated Amorphous-Germanium	8
	2.5.1   Description and working of Hydrogen purifier	8
	2.5.2   Evaporation of Germanium in Hydrogen Environment	9
III.	MEASUREMENT TECHNIQUES	11
	3.1    Thickness measurement	11
	3.2    Gap-width measurement	12
	3.3    Electrical measurement	12
	3.3.1  IV characteristics and d.c. conductivity	12
	3.3.2  Description of the cryostat	14
	3.3.3  Low temperature d.c. conductivity	15
	3.3.4  Annealing and high temperature d.c. conductivity	15

<u>Chapter</u>		<u>Page</u>
IV	EXPERIMENTAL RESULTS	17
	4.1 Electrical properties	17
	4.1.1 Current voltage characteristics	17
	4.1.2 Variation of resistance with air	17
	4.1.3 Effect of hydrogenation on d.c. conductivity	17
	4.1.4 D.C. conductivity of a-Ge-H at low temperature	18
	4.1.5 Annealing of a-Ge	20
	4.1.6 Annealing of hydrogenated a-Ge	20
	4.1.7 Effect of substrate temperature on the conductivity	20
	4.1.8 Effect of rate of deposition on a-Ge-H films	20
	4.2 IR absorption spectrum	21
V	DISCUSSION	22
	5.1 The effect of air exposure on resistance	22
	5.2 Effect of hydrogenation on conductivity	22
	5.3 Variation of conductivity with temperature	23
	5.4 Annealing effect	24
VI	CONCLUSIONS AND SCOPE FOR FUTURE WORK	25
	REFERENCES	42

LIST OF TABLES

	<u>Page</u>
1. Effect of air on resistance.	27
2A. Data of Amorphous Germanium.	28
2B. Data of Hydrogenated Amorphous Germanium.	29
3. Conductivity data of a-Ge and a-Ge-H for different partial pressures	30
(A) Substrate at room temperature.	
(B) Substrate at higher temperature.	
4. Density of states of a-Ge-H for different partial pressures of hydrogen.	31
5. Activation energy of a-Ge-H for different partial pressures of hydrogen.	31
6. Effect of Annealing on a-Ge-H films.	32
7. Conductivity of a-Ge for different substrate temperature.	33
8. Conductivity of a-Ge-H for different rate of deposition.	33

LIST OF FIGURES

	<u>Page</u>
2.1 Hydrogenation system.	6A
2.2 Schematic of sample geometry.	6B
3.1 Schematic of thickness measurements.	6B
3.2 Circuit used for conductivity measurements.	6B
3.3 Cryostat used for low and high temperature conductivity measurements.	14A
4.1 Effect of air on resistance.	17A
4.2 Low temperature conductivity of a-Ge at different $P_H$ .	18A
4.3 $\frac{1000}{T}$ vs conductivity of a-Ge at different $P_H$ .	18B
4.4 Annealing of a-Ge-2.	20A
4.5 Annealing of hydrogenated a-Ge.	20B

## ABSTRACT

Electronic devices at present are only available in the crystalline form of semiconductors as they can be easily doped. The doping of pure a-Ge has been so far unsuccessful because of large number of density of states in the gap. This number may be minimized by increasing the substrate temperature during evaporation or by annealing after evaporation. But to-date annealing is not able to suppress their contribution sufficiently. In case of a-Si the incorporation of hydrogen has been found to be more effective than the heat treatment. In this study these films of a-Ge-H were prepared by evaporating germanium in hydrogen atmosphere at different partial pressure of hydrogen. An attempt was made to characterize the material by studying their, <sup>electrical</sup> properties and by IR spectroscopy.

a-Ge films were prepared under different conditions, and their properties were studied in-situ after exposure to air and after annealing. Among the various parameters varied during preparation were the partial pressure of  $H_2$ , the substrate temperature and the rate of evaporation.

Air at increasing pressure decreased the resistance and hence increased the conductivity of the a-Ge-H samples. Whereas higher substrate temperature, slow deposition rate, higher percentage of hydrogen incorporation and annealing decreased the room temperature conductivity.

Hydrogen incorporation decreased the conductivity by at room temperature of amorphous-germanium by a factor of

toor. for the film deposited at  $75^{\circ}\text{C}$ .

Low temperature conductivity measurements of a-Ge can be explained by variable range hopping at fermi level. For a-Ge-H it can be understood in terms of hopping at band tails.

IR absorption spectrum was studied to find the structural properties of the films. Perhaps due to the small thickness of films no Ge-H peak was observed in evaporated a-Ge-H samples.

These results are favourable but yet not so good as obtained by the glow discharge of germane. Evaporation of germanium in hydrogen plasma has been found to give better results in comparison to the molecular hydrogen.

## CHAPTER I

### INTRODUCTION

An International Conference on Tetra-hedrally Bonded Amorphous Semiconductors was held at the IBM Thomas J. Watson Research Centre, Yorktown Heights, N.Y. from 20th to 22nd March, 1974 [1]. The subject matter of the conference was limited to the physics of amorphous silicon, germanium and related group IV semiconductors. Late in 1975 Spear and LECOMBER [2] announced that they <sup>had</sup> succeeded for the first time in doping amorphous-silicon. This opens up the possibility of fabricating low cost electronic devices. Since then the interest in the subject has been growing at <sup>an</sup> exponential rate. The possibility of using a-semiconductor in solar cell has also been a still more driving force.

Amorphous materials have larger entropy as against the crystalline state. In order to make the material disordered an excess of energy has to be 'frozen in' to the system. Hence to make a material disordered it has to be quenched either from liquid phase or vapour phase. Fast cooling called as 'Splat-Cooling' doesn't give any time to the system to organize itself in the minimum energy state. However a-Ge cannot be obtained by cooling <sup>to liquid phase</sup>. It can be prepared in the following ways:

- (a) Evaporation in vacuum
- (b) R.F. sputtering in argon atmosphere.
- (c) Glow discharge decomposition of germane.

- (d) Electrolytic deposition
- (e) Ion bombardment of crystalline semiconductors

Amorphous materials are also called non-crystalline, glassy or disordered. Amorphous films as they are deposited in vacuum, usually contain large quantities of dangling bonds

in voids and on surfaces. The size of the micro-void ranges from a few angstrom to a few hundred angstrom. The presence of these voids has been established by transmission electron microscopy [3, 4], x-ray scattering [5, 6] and electron scattering [7, 8]. Also these bonds have been observed in ESR experiments [9]. The characteristics of amorphous state in the absence of long range order (LRO) although the short range order (SRO) is present. The nearest neighbour distance and bond angles are found to be almost same (within 10 % of the crystalline value).

Although amorphous semiconductor do not have LRO yet they have bands of non-localized electronic states each separated by mobility gaps. The states within the mobility gap are localized whereas states which are of higher energy or lower energy are extended. It is called as the mobility gap since the mobility of the carriers drops by several order of magnitude at the edges of this gap. These edges are also called valence and conduction band in analogy with the crystals. The concept of density of states is also valid for amorphous materials [10]

The high concentration of localized states in the mobility gap [11], i.e. near the fermi level pins it effectively.

Thus fermi-level is unable to move due to addition of impurities or change of temperature and hence makes the material insensitive to doping. In order to dope the material effectively reduction of these localised states is essential.

The density of state can be reduced by increasing the substrate temperature [12] during evaporation and also by annealing. Higher substrate temperature during evaporation reorganizes the network and eliminates the voids [13]. Decrease in the density of states due to annealing is also interpreted [11, 14] as decrease in the 'voids' or 'dangling bonds' of the deposited film. Removal of dangling bonds has been evidenced by the absence of ESR signal [11, 15]. However deposition of the film on higher substrate temperature and then annealing it also does not make it sensitive for doping in most of the cases.

So, for only a-Si prepared by glow discharge of  $\text{SiH}_4$  at higher substrate temperature has been reportedly doped [2]. Even a-Ge prepared by glow discharge of germane has so far not have been efficiently doped [16]. However doping is possible because these films contain very few localized states in the mobility gap and the success story is due to hydrogen. The localized states formed by dangling bonds which cause the low resistivity of sputtered and evaporated film, gets saturated by the presence of nascent hydrogen during deposition of glow discharge samples [17] and hence <sup>are</sup> able to sweep clear the gap [18, 19]. From IR measurements it has been confirmed that these films contain significant amount of hydrogen (10 % to 35 %) [20].

However, the amount of hydrogen present in these films is much more than the amount required for the compensation of dangling bonds and hence must be changing the atom-network also. The mechanism of hydrogen incorporation is yet not completely understood as it depends on the various deposition parameters but for the controlled fabrication of the devices it is absolutely necessary to understand the complete effect of introducing hydrogen.

The success in doping the a-Si prepared by glow discharge suggests that hydrogenation might be more suited for reducing the dangling bonds than heating. An attempt was therefore made to prepare a-Ge in hydrogen atmosphere at different partial pressures and to study its electrical properties. The effect of deposition parameters, <sup>e.g.</sup> substrate temperature and evaporation rate were also studied. Few samples were annealed to study its effect on a-Ge-H film.

The conductivity of a-Ge films prepared in vacuum was of the order of  $10^{-2} \text{ ohm}^{-1} \text{cm}^{-1}$ . A decrease in the conductivity of a-Ge-H film was observed in the range of  $10^{-3} \text{ ohm}^{-1} \text{cm}^{-1}$  to  $10^{-7} \text{ ohm}^{-1} \text{cm}^{-1}$  i.e. change varied from an order to five orders by using different deposition parameters. Higher substrate temperature and slow deposition rate during evaporation and annealing the sample afterwards were found to be favourable for reduction of density of states near fermi levels. However samples made at increasing partial pressure of hydrogen did not contain hydrogen in increasing magnitude which is not in agreement with

the results obtained by sputtered films [19]. It has been found that smaller the conductivity of the sample greater is the hydrogen incorporation into the film [19]. In sputtered film it was calculated to be 6.5 % for a-Ge-H prepared at  $P_H = 5 \times 10^{-5}$  torr and having the conductivity  $4.7 \times 10^{-7} \text{ ohm}^{-1} \text{cm}^{-1}$ .

The estimate of the absolute hydrogen concentration in Ge-H bonds obtained from absorption coefficient vs photon energy [1]. However, no IR absorption was observed in the evaporated a-Ge-H films in our case, perhaps due to the small thickness. although decrease of conductivity indicates incorporation of hydrogen.

In chapter II, the sample preparations of a-Ge and a-Ge-H are described. In chapter III, the various techniques used for measurements are given. Results are listed in chapter IV and discussed in chapter V. In the last chapter VI conclusions and scope for future work has been discussed.

## CHAPTER II

### SAMPLE PREPARATION

#### 2.1 INTRODUCTION

This chapter deals with the methodology used for the preparation of amorphous-germanium and hydrogenated-amorphous germanium.

#### 2.2 SUBSTRATE CLEANING PROCEDURE

The micro slides of size 25 mm length, 10 mm width and 2 mm thickness were used as substrates. These glass substrates were cleaned in the following manner:

1. Gross dirt was removed by detergent wash and then by ultrasonic wash in 1% detergent solution (phosphate free NaOH) for five minutes.
2. Rinsed in deionised water.
3. Sample was then cleaned ultrasonically in dilute chromic acid for five minutes.
4. Again rinsed in deionised water.
5. Next, samples were ultrasonically cleaned in acetone for 5min.
6. Finally, vapour degreasing of the sample using isopropyl alcohol was done.

#### 2.3 ELECTRODE DEPOSITION

Gold-chrome was used for electrical contacts. The electrodes were formed in a planner geometry with a gap of 0.08 cm and in some cases 0.06 cms as shown in Fig. 2.2

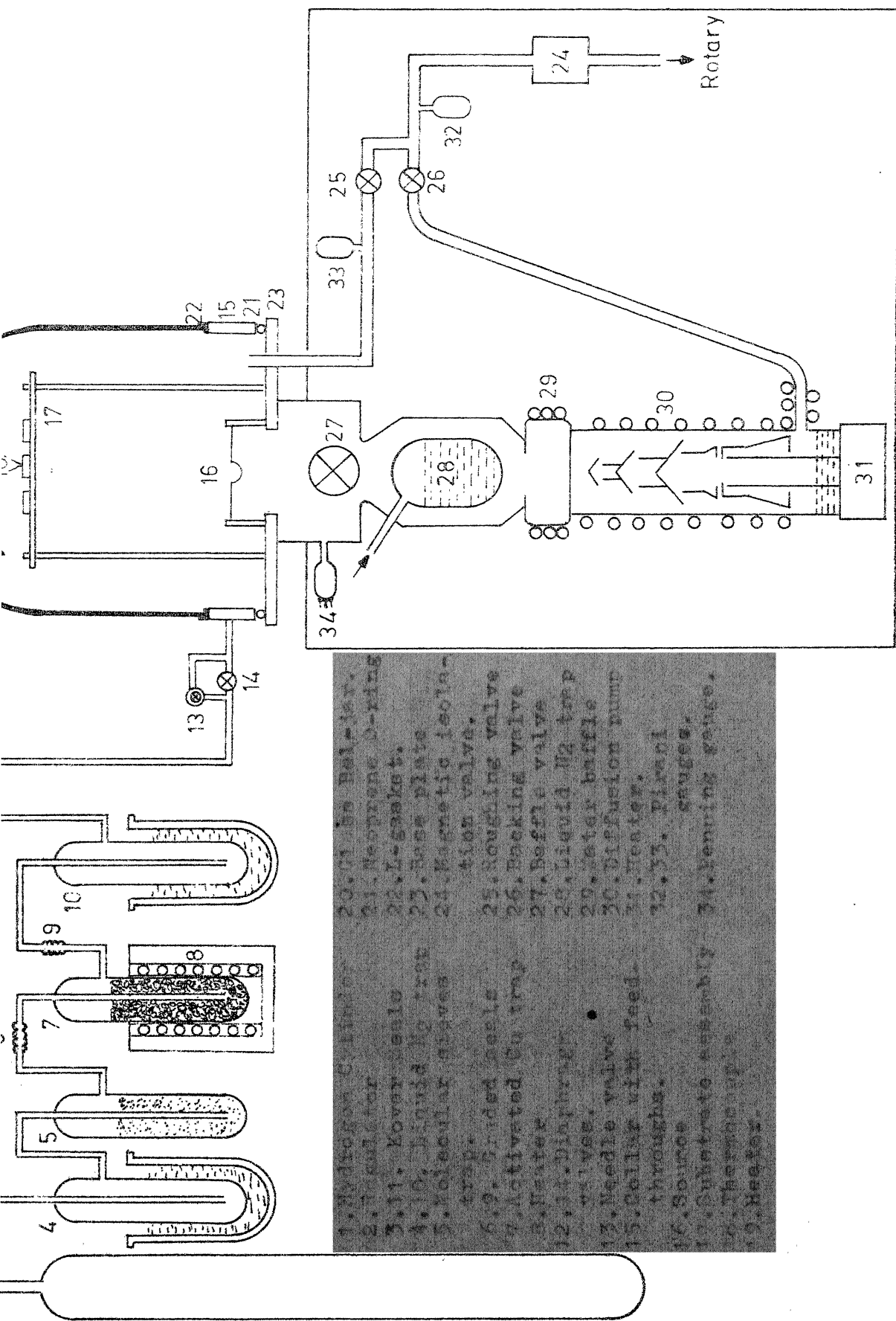


Fig. 2.1 Hydrogenation system

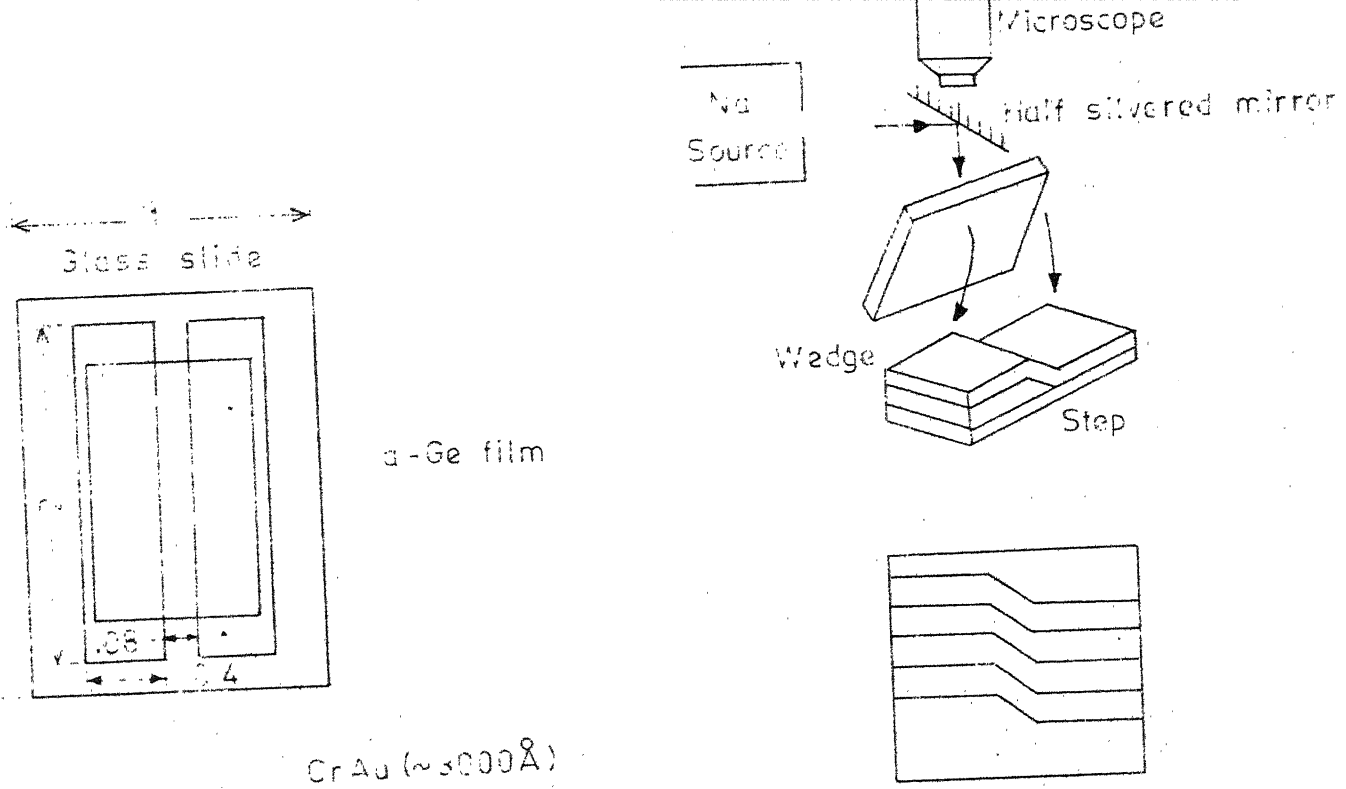


Fig. 2.2 Gap electrode geometry.

Fig. 3.1 Fringe pattern

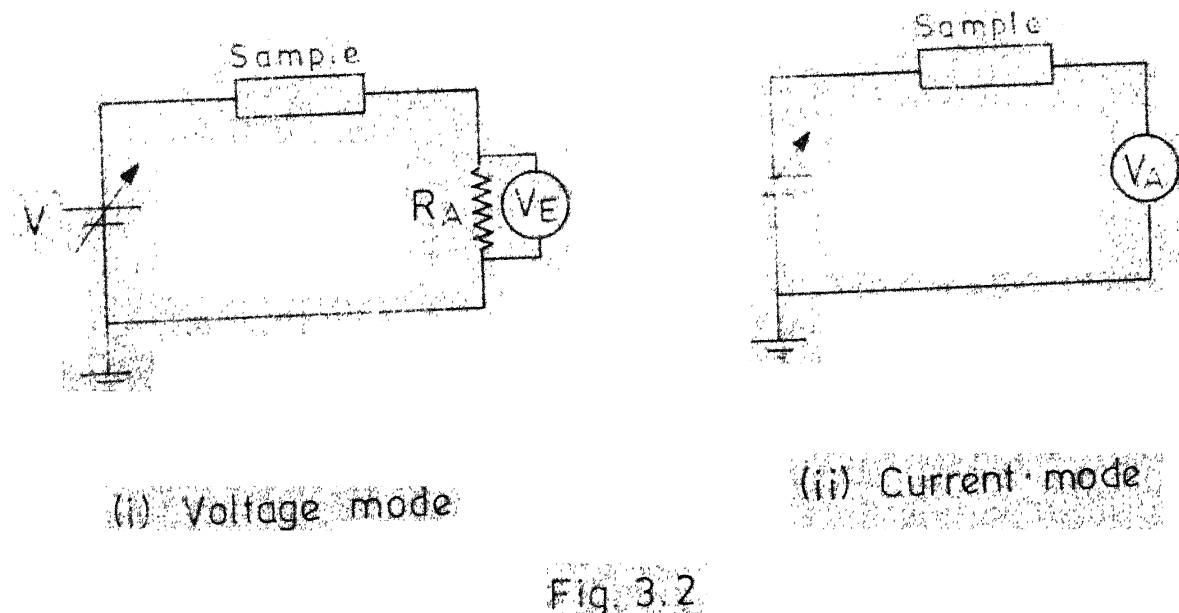


Fig. 3.2

Properly cleaned glass substrates were put into evaporation chamber (17, Fig. 2.1). Evaporation was performed in Vico High Vacuum Coating Unit. Before evaporation system was baked for about an hour using IR lamps and degassing of the boats was done by heating them and then a pressure better than  $5 \times 10^{-6}$  torr was obtained. A tungsten basket was used for chromium and a tungsten filament in the form of helix was used for evaporating gold. The planner geometry was obtained using nichrome strips of 0.08 cms and 0.06 cm thicknesses. The chromium was first evaporated on to hot substrates to obtain a film of approximately 1000  $\text{\AA}$  thickness and then gold was evaporated on top of the chromium film to about a thickness of 2000  $\text{\AA}$ . Chromium is evaporated first because it forms an oxide bond with the glass and hence better adhesion in contrast to the gold which has poor adhesion to the glass. This procedure gives electrodes which stick better to the substrate. Both the evaporations were performed in a single run without breaking the vacuum, using two pairs of electrodes provided in the chamber for the purpose. The pressure during evaporation remained constant.

#### 2.4 DEPOSITION OF AMORPHOUS-GERMANIUM

Amorphous germanium was made by evaporating 99.999 % pure germanium from a tungsten boat. The glass substrate with predeposited electrodes were put above the boat at a distances of approximately 18 cms as shown in Fig. (17, Fig. 2.1). Evaporation was performed at a base pressure

better than  $5 \times 10^{-6}$  torr. Before each evaporation the system was baked and degassing of the boat was also done. The typical evaporation rate was  $\approx 2 \text{ \AA/sec.}$  Germanium evaporation was done with L.T. current of  $\approx 150$  amperes. These films were kept in a desecator immediately after removal from the evaporation chamber.

## 2.5 DEPOSITION OF HYDROGENATED AMORPHOUS GERMANIUM

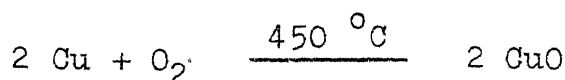
The apparatus used for deposition of hydrogenated a-Ge is shown in Fig. 2.1.

### 2.5.1 Description and working of $\text{H}_2$ -purifier

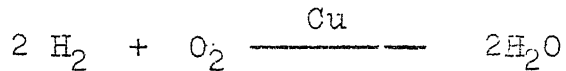
Hydrogen from cylinder is first introduced to a liquid nitrogen trap (4). This trap is kept at liquid nitrogen temperature by putting a liquid nitrogen dewar around it. The impurities with a higher boiling point than that of liquid nitrogen (77 K) are trapped in this. This trap is made of pyrex glass.

Next is a trap containing molecular sieves (5). Molecular sieves absorb the remaining moisture in the hydrogen. This trap is also made of pyrex glass.

After molecular sieves hydrogen is passed to an activated copper trap (7) made of quartz tube and joined on either side by graded seals (6,9) with pyrex tubes. Activated copper is oxygen free. This oxygen free copper reacts with oxygen at  $450^\circ\text{C}$  and makes copper-oxide as follows :



Also, there is a probability of getting water vapour from hydrogen and oxygen in the presence of copper as catalyst



Therefore, after copper-trap hydrogen is free from any traces of oxygen. The trap is kept at  $450^{\circ}\text{C}$  by using a heater (8) around it and applying 130 V by a variac.

Finally, to get rid of water vapour which might have formed in the copper-trap, one more liquid nitrogen trap(10) is added by us in the existing purifier system. This trap is also kept at liquid nitrogen temperature by putting a dewar containing liquid nitrogen around it and hence water vapours are trapped here. This trap is also made of pyrex glass.

For better regulation of hydrogen into the chamber a parallel combination of needle value (13) and diaphragm value (14) is also added by us in addition to the existing diaphragm value (12) glass to metal joints are made of Kovar seals (3,11).

## 2.52 Evaporation of Ge in He environment

The whole system including hydrogen purifier was initially evacuated using the rotary pump to a pressure of  $5 \times 10^{-2}$  torr with both the diaphragm values (12, 14) and needle value (13) open. The evaporation units and hydrogen purifier unit including molecular sieves and liquid nitrogen traps were

baked using IR lamps. Copper turnings were activated by applying ~130 Volts from a variac to the heater (8) for two hours. The roughing valve (25) was closed first and then the backing valve (26) was opened. Lastly, the baffle valve (27) was opened to connect the diffusion pump to the chamber.

In the first case, <sup>With the</sup> diffusion pump on and needle valve (13) and diaphragm valve (14) both open the pressure was  $5 \times 10^{-6}$  torr. The pressure in the second case when only needle valve (13) is open while diaphragm valve (14) <sup>was</sup> closed again  $5 \times 10^{-6}$  torr. But in the third case when both the needle and diaphragm <sup>valves</sup> were closed the base pressure was better than  $5 \times 10^{-6}$  torr. Purified hydrogen from the purifier was then introduced in to the chamber which was already at the base pressure of  $5 \times 10^{-6}$  torr. The flow of hydrogen was controlled using the needle valve (13) to get the desired pressure in the range of  $2 \times 10^{-4}$  torr to  $5 \times 10^{-5}$  torr.

The vacuum chamber was flushed with hydrogen for an hour and then germanium evaporation was done on glass substrates with predeposited electrodes as described in Section 2.4. Also KBr pellets for Infra-Red measurements and clean glass substrates for thickness measurements were kept along with the predeposited electrodes. Arrangements for in-situ electrical conductivity measurements were also done through collar feed throughs.

After the deposition, hydrogen flow was stopped and the system was evacuated to again to a base pressure of  $< 5 \times 10^{-6}$  torr. After introducing air into the chamber samples were taken out and were immediately kept in the desecicator.

## CHAPTER III

### MEASUREMENT TECHNIQUES

#### 3.1 THICKNESS MEASUREMENT

The thickness of the  $\alpha$ -germanium and hydrogenated  $\alpha$ -germanium films was measured by Tolansky method (21). The optical microscope made by CENSISCO-3066 was used along with an eyepiece - Meopta 219206.

The basic principle is to divide the intensities of a monochromatic light beam by a half silvered mirror and then after multiple reflections the fringe pattern is formed which is viewed through the microscope as shown in Fig. 3.1. Here sodium lamp was used as a monochromatic source of light with average wavelength  $5893^{\circ}\text{A}$ .

For thickness measurements the samples were deposited on to a glass slide in such a way that they covered half the length of the glass slide. Then a wedge is formed by putting thin hair so as to lie in the clean and deposited portions of the glass slide simultaneously. Due to the formation of step fringe pattern also gets shifted at the edge. Then

$$t = \frac{n\lambda}{2}$$

where

$t$  = thickness of the film.

$n$  = number of fringes shifted.

$\lambda$  = wavelength of the monochromatic light.

Now, to get the number of fringes shifted fringe width is obtained on the micrometer scale and is then divided by shift of fringes on the same scale reading. Hence, the final formula used for the thickness is

$$t = \frac{w}{s} \times \frac{\lambda}{2}$$

where

w = fringe width

s = shift of the fringes

### 3.2 GAP WIDTH MEASUREMENT

Gap width is the distance between the electrodes. It is measured with the same microscope CENISCO-3066 in the ordinary way. In the micrometer scale 1 mm is divided into 8 equal divisions. Hence from scale reading gap-width is calculated in cms.

### 3.3 ELECTRICAL MEASUREMENTS

#### 3.3.1 IV Characteristics and d.c. conductivity

Current voltage characteristics were studied by using a regulated variable power supply (aplab Type LVA 100/-5 a aplab Model 7112), a DC - Microvoltmeter (Philips - Pp9004) and an electrometer amplifier (ECIL Model EA815 or Keithly 610). The electrometer amplifier was used both in voltage and current mode.

In voltage mode (ECIL Model), the electrometer amplifier was used with an input impedance of  $10^{12}$  ohms and the voltage

drop across a precision resistor (100 K ohms  $\pm 0.01$  percent) was measured. Similarly, in normal mode of Keithly voltage drop across  $10^5$  ohms or  $10^6$  ohms known resistance was measured. Resistance of the sample was calculated by the formula.

$$R_s = \frac{\text{applied voltage} - \text{potential drop across the known resistance}}{\text{potential drop across the known resistance}} \times \text{known resistance}$$

The Keithly electrometer in normal mode was also used to measure the current directly. For this the input resistance of the meter was chosen at least two orders less than the sample resistance, so that the potential drop across the known resistance of the meter becomes negligibly small and the potential drop was mainly across the sample. Knowing the applied voltage and the current in the circuit the resistance of the sample was also easily calculated.

For conductivity measurements resistance of the sample is obtained from the IV measurement. The distance between the two electrodes, length of the sample and thickness of the film was obtained optically and substituted in the following formula.

$$\sigma = \frac{d}{R_s \cdot t \cdot l} \text{ ohm}^{-1} \text{ cm}^{-1}$$

where

$\sigma$  = conductivity of the sample.

$d$  = distance between the electrodes (gap-width)

$R_s$  = resistance of the sample

$t$  = thickness of the sample

$l$  = length of electrode in contact with the sample.

### 3.3.2 DESCRIPTION OF THE CRYOSTAT

The cryostat (Fig. 3.3) used for low and high temperature measurements consists of a brass substrate holder (15) on to which the sample is held in position by two phosphor bronze clips (2). These clips are fixed by two teflon screws (3) to the substrate holder. The temperature is measured by a chromel-alumel thermocouple (5) [ one of the cryostat which has arrangement for low temperature measurements only, has copper constantan thermocouple. For <sup>a</sup> few samples this cryostat was also used.] The junction of the thermocouple is clamped to the top of the glass plate of the same thickness as that of the sample. The current leads (4) come out of the flange (13) through teflon connector (6), whereas thermocouple leads (5) and heater leads (17) come out of the flange through glass to metal feedthrough (14). The substrate holder is covered by a pyrex dewar (10) with flange which sits on the O-ring (12), to the ground metal flange (13).

The dewar is evacuated by a rotary pump through the opening (7), ~~and the pressure is measured by a thermocouple (1BP torr) gauge through the opening (7),~~ and the pressure is measured by a ~~thermocouple (1BP torr) gauge through the opening (7),~~ Pirani gauge through the opening (8) the whole system is put in a double walled dewar. The space between dewars (10, 11) is used to fill liquid nitrogen (16) for low temperature measurements and instead heater (17) is used for high temperature measurements.

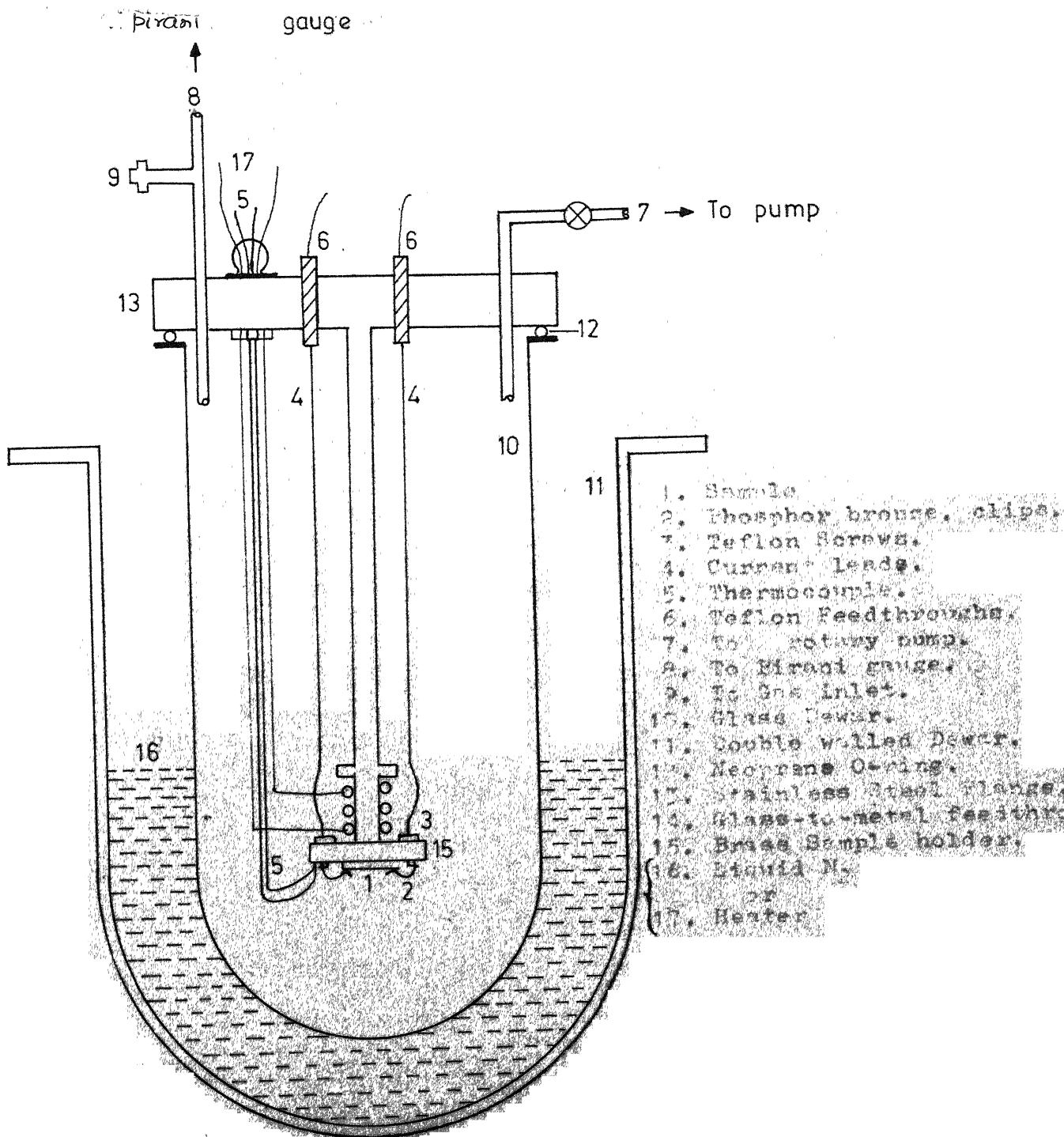


Fig. 3.3 Cryostat used for low and high temperature conductivity measurements.

### 3.3.3 Low Temperature d.c. conductivity

For low temperature d.c. conductivity measurements the samples were loaded in a cryostat as shown in Fig. 3.3. The cryostat has been described in the above section 3.3.2. The circuits and the formula for d.c. conductivity measurements were same as that of IV characteristic and d.c. conductivity of section 3.3.1.

After loading the dewar (10) was evacuated by a rotary pump to a pressure of about  $2 \times 10^{-2}$  torr. The temperature was lowered by pouring liquid nitrogen in steps into the space between dewars (10, 11). Different levels of nitrogen in this space give different temperature. Hence at different levels of liquid nitrogen, the temperature was allowed to stabilize and then only observations were taken. The range of measurement done by this apparatus was from room temperature to 170 K (-130 °C).

### 3.3.4 Annealing and high temperature d.c. conductivity

The apparatus used for annealing and high temperature d.c. conductivity measurements is shown in Fig. 3.3. It was same as used for low temperature d.c. conductivity measurements with a difference that here heater terminals (17) were used instead of liquid nitrogen (16). The description of the apparatus has already been given in the section 3.3.2.

The measurements were made by using the annealing apparatus, a variable power supply, microvoltmeter and an electrometer.

amplifier. For heating the coil (17) another power supply or a variac was used. The sample was loaded and dewar(10) was evacuated to a rotary pressure of  $2 \times 10^{-2}$  torr. Then current was passed through the heating coil (17) so that the desired temperature was reached. Temperature was measured in thermo e.m.f. by the microvoltmeter across the thermocouple (5). At stable temperature conductivity measurements were made. The current through the heating coil is then increased in steps and at each step temperature was allowed to stabilize and measurements were made. In studying the sample a-Ge (2) current was passed in single step to obtain the desired maximum temperature. At the maximum temperature the sample is heated for an hour and i.e. annealed at that temperature.

After annealing, the current through heating coil was reduced in steps, temperature was again allowed to stabilize and at each static temperature conductivity measurements were made. By this apparatus conductivity was measured from room temperature to about 430 K (approximate 160 °C).

## CHAPTER IV

### EXPERIMENTAL RESULTS

#### 4.1 ELECTRICAL PROPERTIES

##### 4.1.1 Current Voltage characteristics

Initially for all the samples ohmic nature was tested. Most of the a-Ge and a-Ge-H films were found to be ohmic upto electric field  $10^3$  volt/cm. Some films were found to be non-ohmic even at a very low field 100 volt/cm. No investigations on such non-ohmic films were carried out.

##### 4.1.2 Variation of resistance with air

The resistance data for hydrogenated a-Ge are shown in Table 1. The resistance was found to decrease by half order for the sample a-Ge-H (2) for the variation of pressure from  $2 \times 10^{-2}$  torr to atmosphere and one third order for the sample a-Ge-H (3). The value of the change of resistance on exposure to environment was same in both the cases. Fig. 4.1 shows the effect of air on resistance.

##### 4.1.3 Effect of hydrogenation on d.c. conductivity

Tables 2(A) and 2(B) summarise almost all the experimental results. The d.c. conductivity for a-Ge was in the range of  $10^{-2} \text{ ohm}^{-1} \text{cm}^{-1}$  whereas hydrogen incorporation decreases the conductivity in the range  $10^{-3} \text{ ohm}^{-1} \text{cm}^{-1}$  to  $10^{-7} \text{ ohm}^{-1} \text{cm}^{-1}$ . The hydrogenation depends on several factors pressure of hydrogen, purity of hydrogen, evaporation rate, substrate temperat

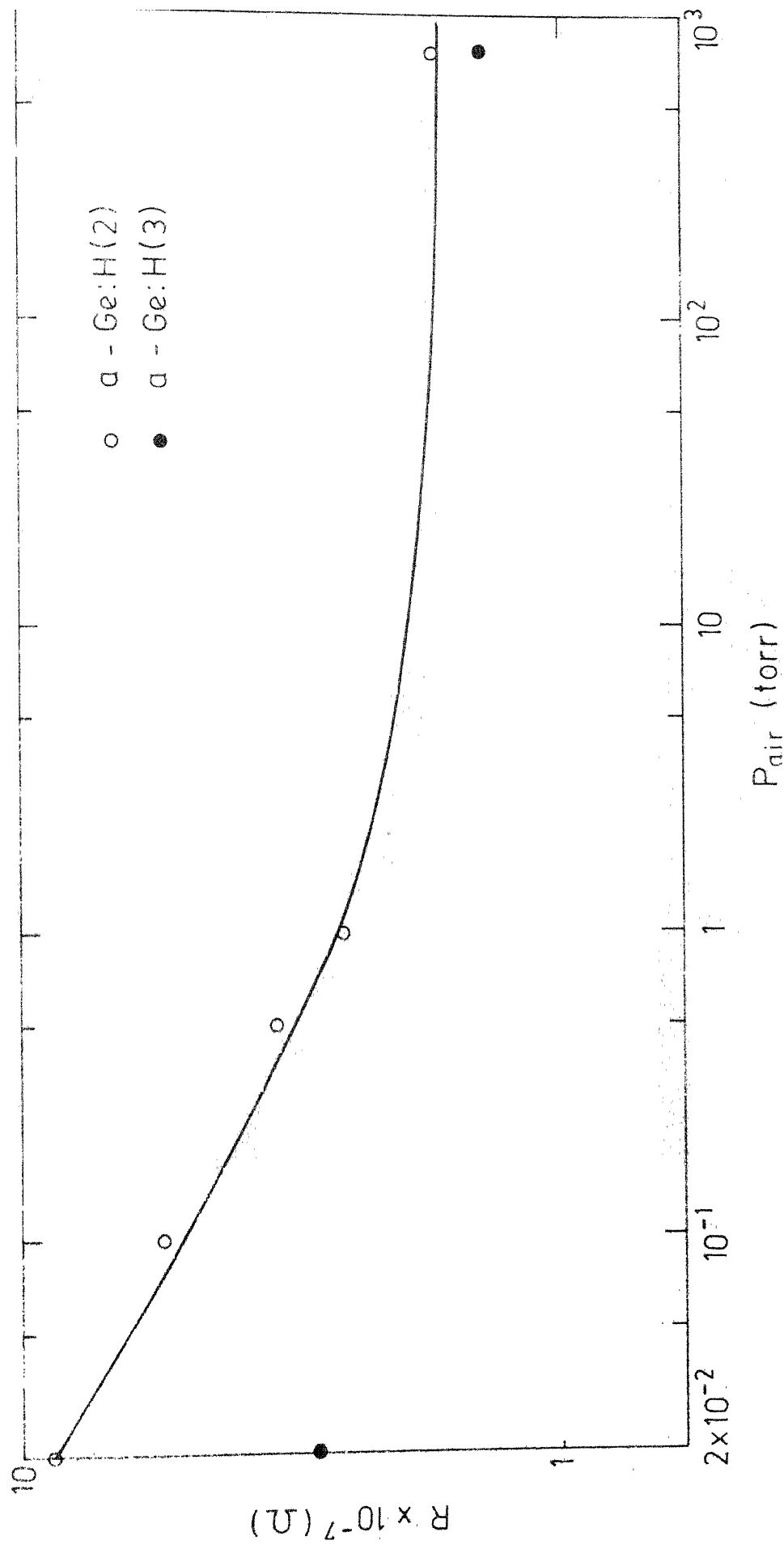


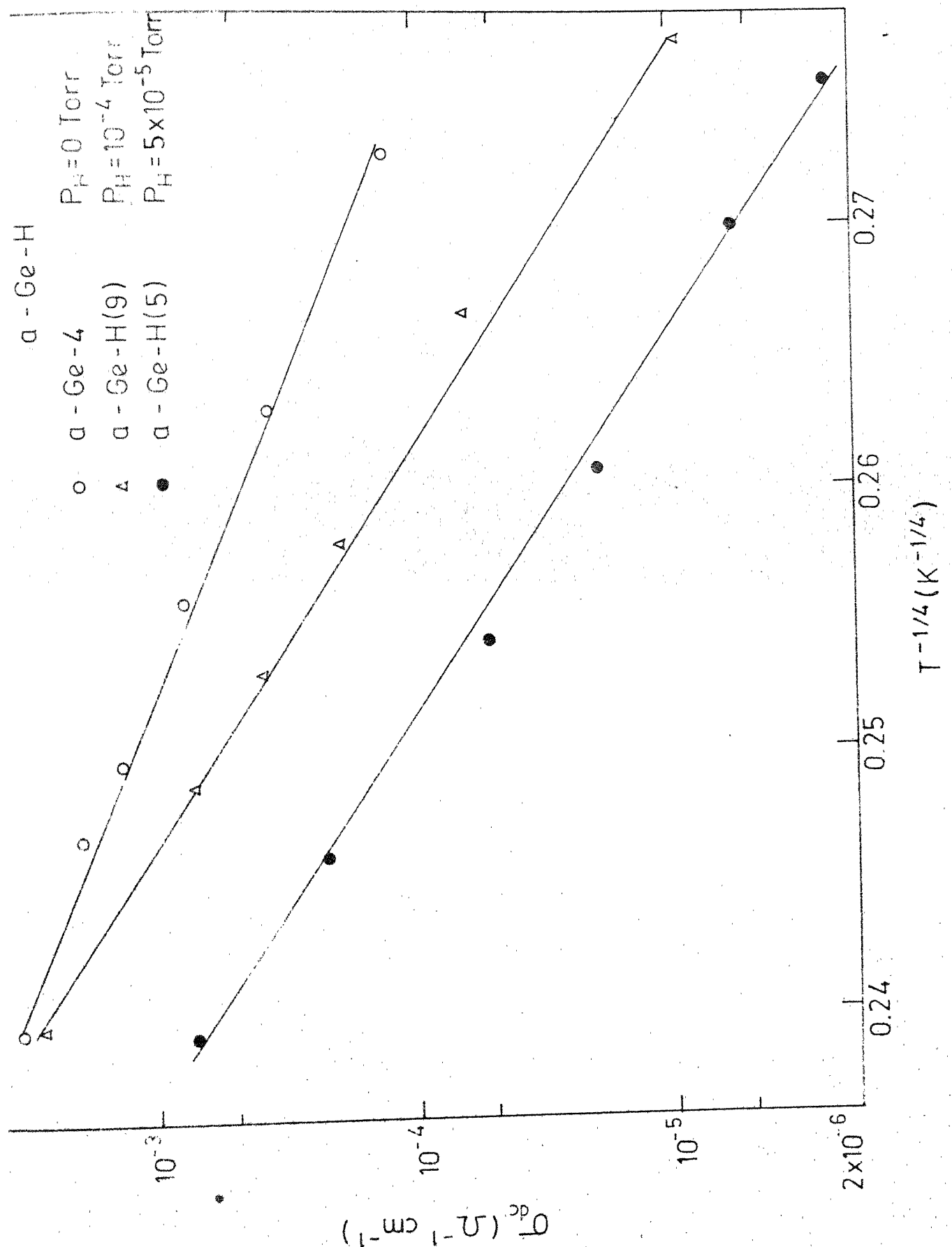
Fig. 4.1 Effect of air on resistance.

time of heating of boat before evaporation and on other not so well defined parameters. However, reproducibility of the results have not been checked.

#### 4.1.4 D.C. conductivity of a-Ge-H at low temperature

The conductivity data for hydrogenated a-Ge with varying partial pressures of hydrogen are shown in Table 3. The increase of partial pressure decreases the room temperature conductivity from  $1.68 \times 10^{-2} \text{ ohm}^{-1} \text{cm}^{-1}$  to  $4.5 \times 10^{-6} \text{ ohm}^{-1} \text{cm}^{-1}$ . However results obtained for higher substrate temperature are not in complete agreement with this. At higher substrate temperature also it has been found that hydrogenation still decreased the conductivity but somehow for lower pressure  $5 \times 10^{-5}$  torr, it was found to be  $7.2 \times 10^{-4} \text{ ohm}^{-1} \text{cm}^{-1}$  and for comparatively higher pressure  $10^{-4}$  torr it was found to be  $2.76 \times 10^{-3} \text{ ohm}^{-1} \text{cm}^{-1}$ .

The variation of conductivity with temperature in low temperature range is shown in Fig. 4.2. In this figure we have plotted  $T^{-1/2}$  vs  $\log \sigma$ . Increase of partial pressure of hydrogen from 0 torr to  $10^{-4}$  torr still gave the straight line obeying Mott's  $T^{-1/4}$  law. In the non-hydrogenated sample conductivity changed from  $3.2 \times 10^{-3} \text{ ohm}^{-1} \text{cm}^{-1}$  to  $1.54 \times 10^{-4} \text{ ohm}^{-1} \text{cm}^{-1}$  when the temperature ~~from room temperature~~ changes from room temperature to 180 K. On the other hand in the hydrogenated sample a-Ge-H (5) evaporated at a partial pressure of  $5 \times 10^{-5}$  torr, conductivity varies from  $7.2 \times 10^{-4} \text{ ohm}^{-1} \text{cm}^{-1}$  to  $2.45 \times 10^{-6} \text{ ohm}^{-1} \text{cm}^{-1}$  and in the sample a-Ge-H (9) evaporated at partial pressure  $10^{-4}$  torr conductivity varies from  $2.73 \times 10^{-3} \text{ ohm}^{-1} \text{cm}^{-1}$  to



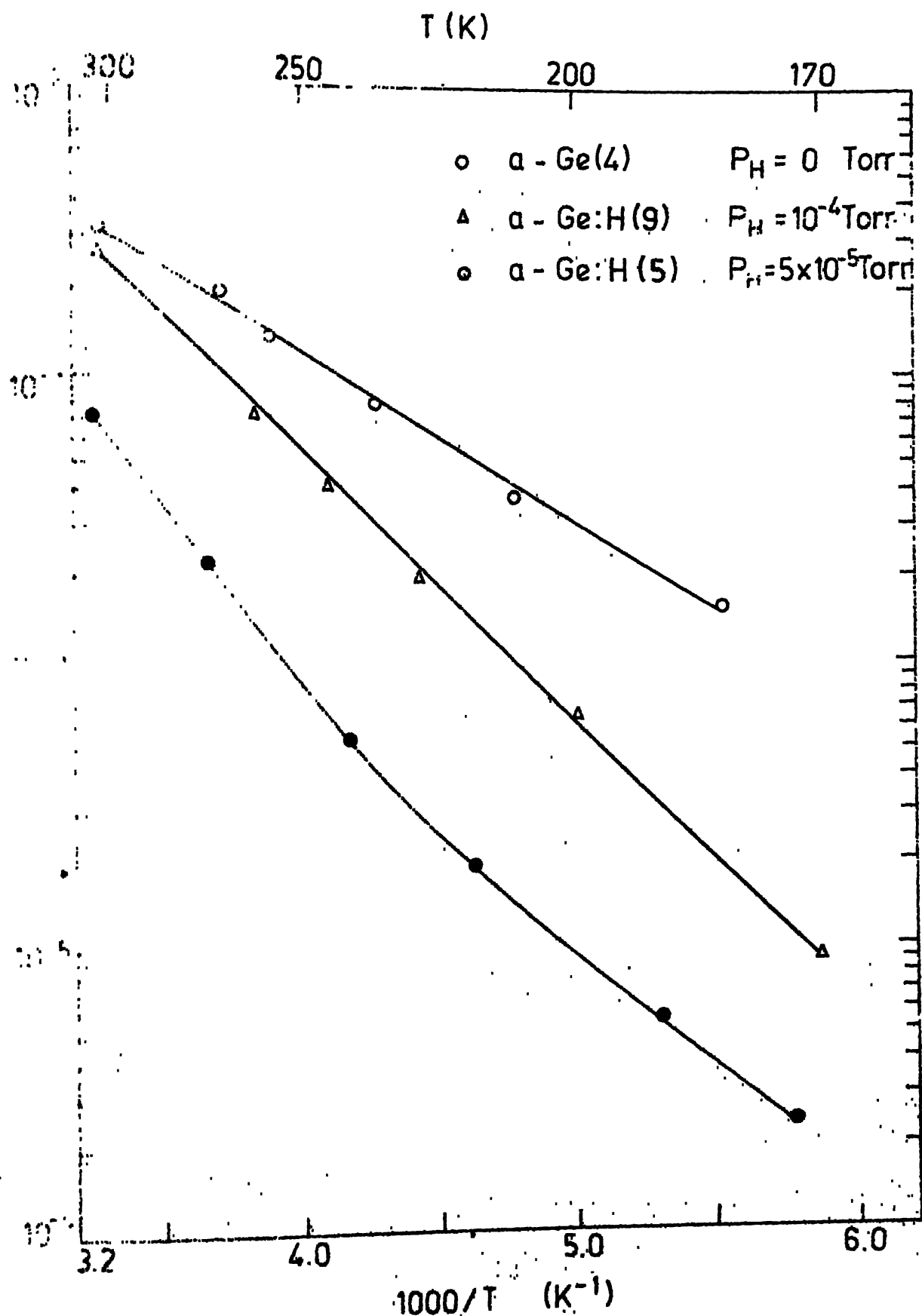


Fig. 4.3:  $1000/T$  vs. conductivity of a-Ge at different  $P_H$ .

$9.08 \times 10^{-6} \text{ ohm}^{-1} \text{cm}^{-1}$  when the temperature changes from room temperature to 170 K. Hence in low temperature range for a-Ge there is only one order change in conductivity whereas for hydrogenated a-Ge the change in the order of conductivity is from two to three orders.

A rough estimate of density of states near the fermi level can be made for the samples which follow Mott's  $T^{-1/4}$  law, using the relation

$$\sigma = \sigma_0 \exp \left( - \frac{T_0}{T} \right)^{1/4}$$

where  $\sigma_0$  and  $T_0$  are Mott's parameter. The density of states is given by

$$N(E_f) = \frac{16 \alpha^3}{kT_0}$$

where  $k$  = Boltzmann constant.

$\alpha$  = localization length.

The results for density of states are listed in Table 4. Calculations were done using  $k = 8.616 \times 10^{-5} \text{ ev/k}$  and  $\alpha^{-1} = 10 \text{ \AA}^2$ . For a-Ge (4) the density of states were  $2.19 \times 10^{18} \text{ cm}^{-3} \text{ ev}^{-1}$  whereas for hydrogenated sample a-Ge-H (5) prepared at  $5 \times 10^{-5}$  torr  $P_{H_2}$  it is  $3 \times 10^{17} \text{ cm}^{-3} \text{ ev}^{-1}$  and for a-Ge-H (9) at  $10^{-4}$  torr  $P_{H_2}$  it is  $3.5 \times 10^{17} \text{ cm}^{-3} \text{ ev}^{-1}$ . Hence hydrogenation decreases the density of states.

#### 4.1.5 Annealing of a-Ge

Fig. 4.4 shows the annealing of a-Ge (2). The data are listed in Table 6. a-Ge (2) annealed at 390 K for an hour shows a change in room temperature conductivity from  $6.9 \times 10^{-3} \text{ ohm}^{-1} \text{cm}^{-1}$  to  $3.01 \times 10^{-3} \text{ ohm}^{-1} \text{cm}^{-1}$ . The same sample was again annealed at higher temperature 430 K which further decreased its conductivity to  $1.36 \times 10^{-3} \text{ ohm}^{-1} \text{cm}^{-1}$ .

#### 4.1.6 Annealing of hydrogenated a-Ge

Annealing of hydrogenated a-Ge has the similar effect on the sample as that on pure a-Ge. Fig. 4.5 shows the annealing effect on hydrogenated amorphous germanium evaporated at different partial pressure of hydrogen. The data are recorded in Table 6. The conductivity for a-Ge (4) decreased from  $3.29 \times 10^{-3} \text{ ohm}^{-1} \text{cm}^{-1}$  to  $1.55 \times 10^{-3} \text{ ohm}^{-1} \text{cm}^{-1}$ . The sample prepared at higher partial pressure of hydrogen a-Ge-H (9) at  $10^{-4}$  torr had more change in the conductivity in comparison to the sample a-Ge-H(5) prepared at  $5 \times 10^{-5}$  torr.

#### 4.1.7 Effect of substrate temperature on the conductivity

Increase in substrate temperature decreases the conductivity. Conductivity for a-Ge (1) sample for which substrate was held at room temperature is  $1.68 \times 10^{-2} \text{ ohm}^{-1} \text{cm}^{-1}$  whereas it decreases to  $3.3 \times 10^{-3} \text{ ohm}^{-1} \text{cm}^{-1}$  for the substrate temperature 340 K as is clear in Table 7.

#### 4.1.8 Effect of rate of deposition on a-Ge-H films

Table 8 shows the effect of rate of deposition. The rate

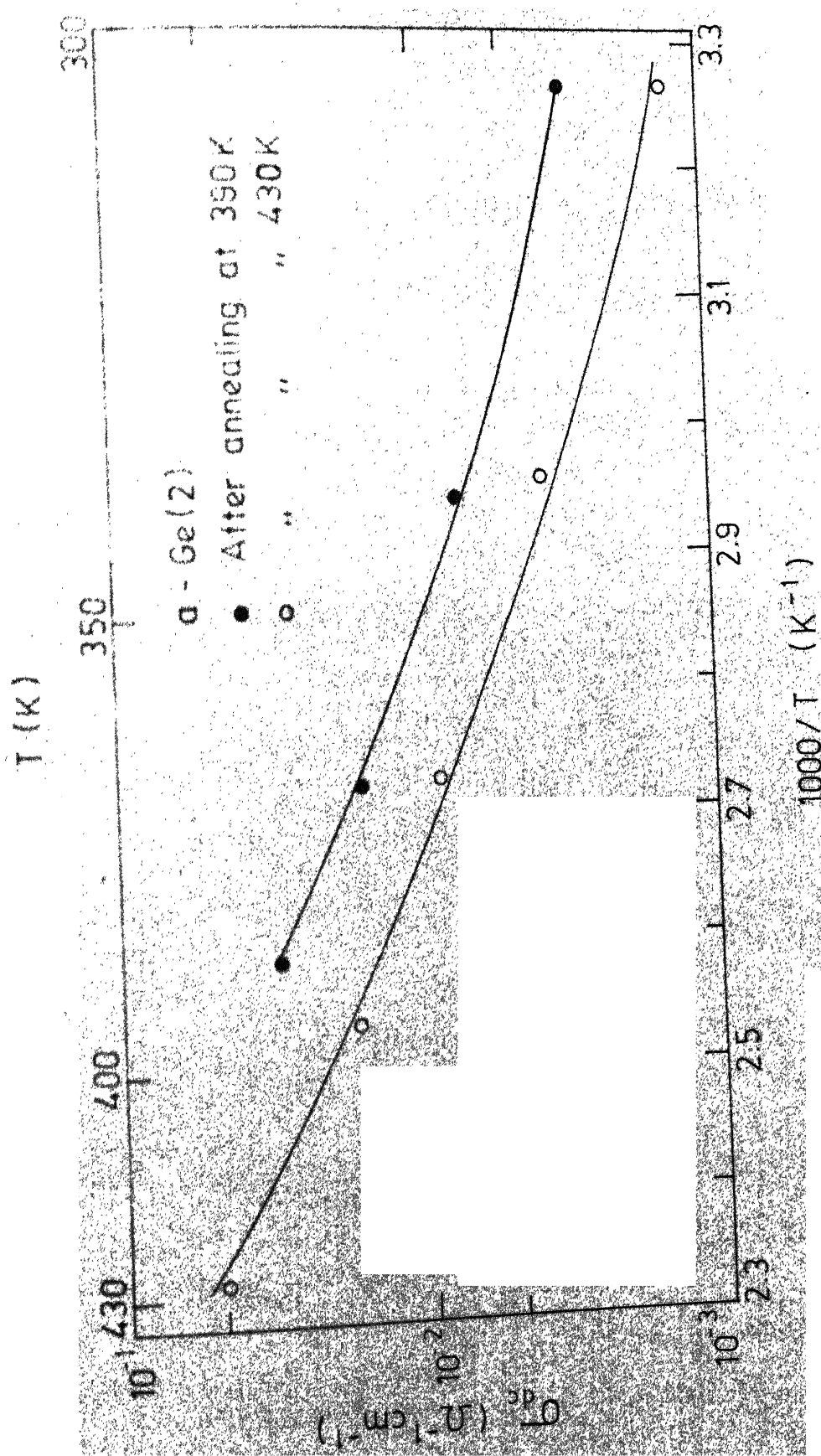


Fig. 4.4 Annealing of  $\alpha\text{-Ge(2)}$

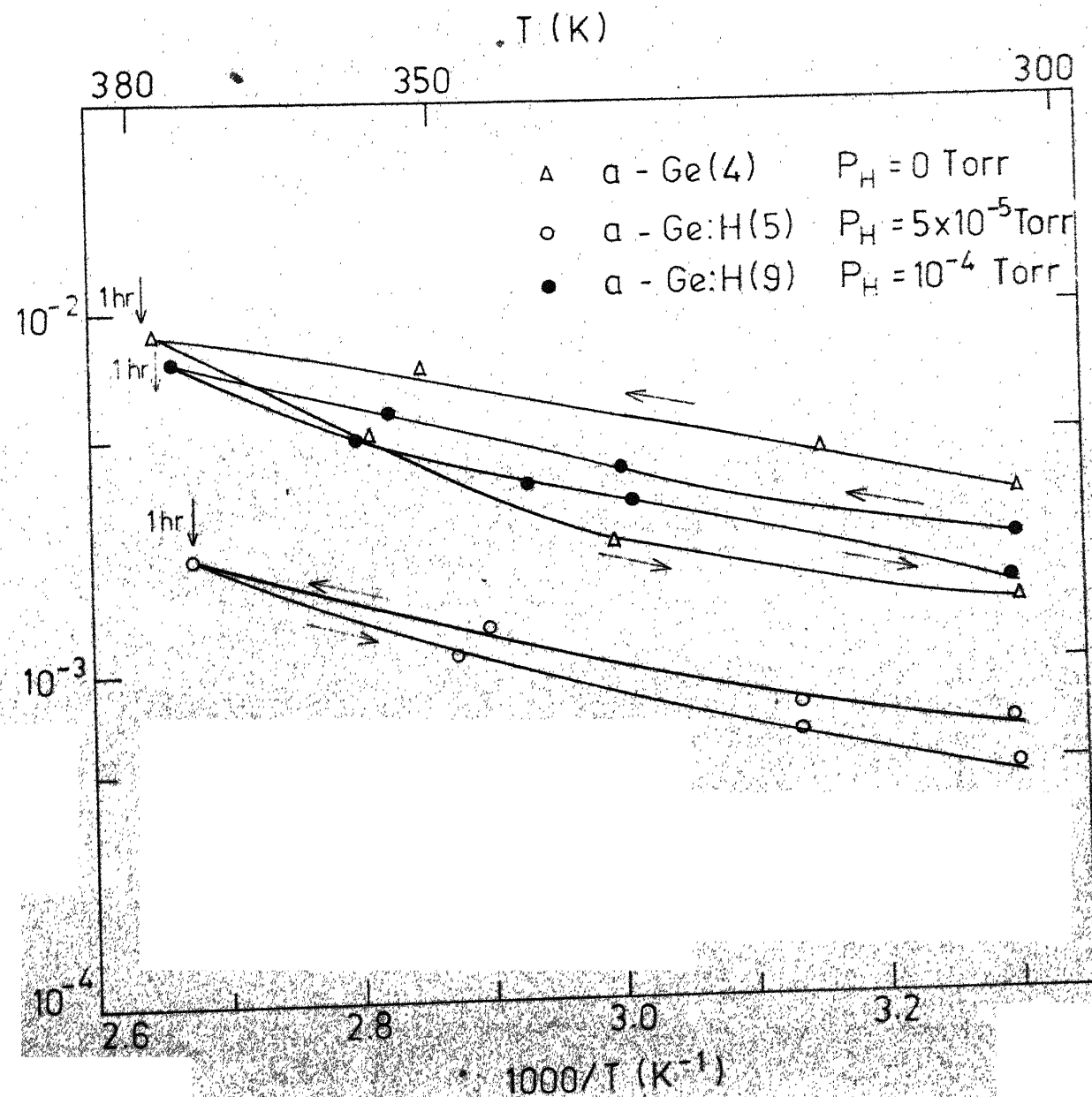


Fig. 4.5 Annealing of hydrogenated  $\alpha$ -Ge

of deposition. is total thickness divided by the time of deposition. The effect was studied on the samples prepared at  $5 \times 10^{-5}$  torr partial pressure of hydrogen. The sample a-Ge-H (4) prepared at very low evaporation rate  $0.444 \text{ \AA/sec.}^{\circ}$ , has the conductivity  $2.23 \times 10^{-7} \text{ ohm}^{-1} \text{ cm}^{-1}$  and for a-Ge-H (5) for which the evaporation rate was higher  $1.56 \text{ \AA/sec.}^{\circ}$  has correspondingly higher conductivity  $7.22 \times 10^{-4} \text{ ohm}^{-1} \text{ cm}^{-1}$ .

#### 4.2 IR ABSORPTION SPECTRUM

$\text{KB}_r$  pellets were used to find out the incorporation of hydrogen in germanium. Ge-H peak is about  $1950 \text{ cm}^{-1}$  for which  $\text{KB}_r$  is transparent. However no Ge-H peak was observed in any of the samples, although effect of hydrogenation is observed in the measurement of conductivity.

perhaps due to the small thickness.

LIBRARY  
Ass. No. A 66963

## CHAPTER V

### DISCUSSION

#### 5.1 THE EFFECT OF AIR EXPOSURE ON RESISTANCE

It has been reported by M. Kastner and H. Fritzsche [22] that for a-Ge resistance decreases as it is exposed to increasing air pressure mainly due to humidity. The resistance decreases because water fills the void and hence makes it more conducting.

The similar effect is observed by us in hydrogenated a-Ge as it is easily understood by the above reasoning.

#### 5.2 EFFECT OF HYDROGENATION ON CONDUCTIVITY

Conductivity of a-Ge decreases with hydrogenation. Howe Lewis et al. [1] studied the sputtered film. V. Kumar [23] & the films by evaporation in hydrogen. The results indicate that conductivity decreases with increase of hydrogen partial pressure during preparation.

By absorption data and ESR studies percentage of hydrogen is calculated in the sample of sputtered film. Greater the hydrogen incorporation lesser was the conductivity of the samples

Hydrogen incorporation is found to decrease the conduct of both the samples a-Ge-H (5) and a-Ge-H (9). However, greater incorporation of hydrogen at lower pressure  $5 \times 10^{-5}$  torr in

a-Ge-H (5) and lesser incorporation of hydrogen at higher pressure  $10^{-4}$  torr in a-Ge-H (9) sample is yet to be understood.

However more experimentation has to be done to say the final word.

### 5.3 VARIATION OF CONDUCTIVITY WITH TEMPERATURE

In low temperature range conductivity for a-Ge and a-Si have been explained by Mott's [24] variable range hopping at the fermi level, whereas for high temperature it is governed by intrinsic conduction mechanism and hence band to band conduction is dominant at high temperature.

For low temperature range this theory is expected to hold at very low temperatures (Helium temperature only) but in a-Ge Mott's  $T^{-1/4}$ -law is well fitted even upto room temperature. In this theory  $\sigma = \sigma_0 \exp(-\frac{T_0}{T})^{1/4}$ , where  $\sigma_0$  and  $T_0$  are the functions of  $N(E_f)$  and several authors [12, 25, 26] have tried to calculate  $N(E_f)$  from  $\sigma$ , fitting their data to  $T^{-1/4}$  but this has always given unreasonable values. However,  $N(E_f)$  calculated from the slope of the  $T^{-1/4}$  vs  $\log \sigma$  straight line along with a suitable choice of  $\alpha$  gives  $N(E_f)$  which appears reasonable [27, 28].

Our results give a straight line for  $T^{-1/4}$  vs  $\sigma_{d.c.}$  and hence are in agreement with the theory. The density

of the states near fermi level reduces from  $2.19 \times 10^{18}/\text{cm}^3/\text{ev}$  to  $10^{18}/\text{cm}^3/\text{ev}$  for the sample a-Ge-H (5) evaporated at pressure  $5 \times 10^{-5}$  torr.

#### 5.4 ANNEALING EFFECT

The deposition of an amorphous film on-to a cold substrate is somewhat similar to a rapid quench; it leaves the material in a structural state of higher energy. Subsequent annealing brings down the structure to its meta stable equilibrium ~~which is nearer to the of the stable state~~ of minimum free energy [29]. The process reduces the number of defects and unpaired spins diminishes the strain and promotes recombination and energetically favourable bonds [30, 31]. As a result an increase in band gap and decrease in density of state within the gap is expected. As a result, annealing decreases the conductivity of the samples.

## CHAPTER VI

### CONCLUSIONS AND SCOPE FOR FUTURE WORK

A study of electrical properties of hydrogenated amorphous germanium films prepared by evaporation in hydrogen atmosphere has been done in this thesis. With the limited experimentation, the following conclusions are drawn from the present investigations.

The d.c. conductivity is found to depend on various deposition parameters such as substrate temperature, evaporation rate and partial pressure of hydrogen. The room temperature conductivity of a-Ge-H increased with the increase of partial pressure in the range of  $10^{-4}$  torr to  $10^{-5}$  torr is yet to be explained after doing more experimentation.

Annealing on a-Ge-H films has the desired effect of reducing the density of states and increasing the activation energy. No effect was observed by IR spectroscopy. This means that the incorporation of hydrogen is very less and it has to be studied for greater thickness of the film to finally comment on it. Only one hydrogenated sample a-Ge-H (4) showed some evidence of photo-conductivity and that too wasn't measurable. Much work has to be done in this field.

The role of hydrogen incorporation into the evaporated germanium can be understood more systematically by doing electron microscopy, IR spectroscopy, ESR and by optimizing various deposition parameters. Effect of discharge and high substrate

temperature while evaporating and also annealing the film in plasma has to be studied more carefully. Perhaps, then the evaporated a-Ge films might become comparable to the glow discharge produced films.

TABLE 1  
Effect of air on resistance

S.No.	Sample	$P_{air}$ Torr	Resistance $\times 10^{-7}$ ohm
1	a-Ge-H(2)	$2 \times 10^{-2}$	8.5
		$1 \times 10^{-1}$	6.7
		$5 \times 10^{-1}$	4.9
		1	3.7
		atmosphere	3.2
2.	a-Ge-H(3)	$2 \times 10^{-2}$	5.1
		atmosphere	2.3

TABLE 2(A) (Amorphous Germanium)

S.No.	Sample No.	At room temperature		$\frac{\Delta E}{E_F}$	Evaporation rate	Remarks
		Pressure	$\sigma_{air}$			
1.	a-Ge-1	$5 \times 10^{-6}$ Torr	$1.68 \times 10^{-2}$ ohm $^{-1}$ cm $^{-1}$	$8.72 \times 10^{-18}$ cm $^{-2}$ (ev) $^{-1}$	$0.15 \text{ ev}_{(at 300^{\circ}\text{K})}$ $0.067 \text{ ev}_{(at 180^{\circ}\text{K})}$	$\frac{2945}{15 \times 60} = 3.272$ ohmic
2.	a-Ge-2	$5 \times 10^{-6}$	-	$6.9 \times 10^{-3}$	(a) 0.41 ev (b) (after annealing) (temp. 390 K) 0.193 ev (temp. 300 K) $\frac{2550}{15 \times 60} = 2.833$ ohmic	
3.	a-Ge-3	$5 \times 10^{-6}$	-	-	$\frac{2200}{10 \times 60} = 3.66$	Non-ohmic
4.	a-Ge-4	$5 \times 10^{-6}$	$3.25 \times 10^{-3}$	-	$2.19 \times 10^{-18}$	ohmic
					$\frac{1955}{15 \times 60} = 2.1853$	High subrate $t_{\text{sub}}$ 340 K.
					$0.12 \text{ ev}$	

TABLE 2(B) (Hydrogenated Amorphous Germanium)

S. No.	Sample No.	Partial pressure of H <sub>2</sub> in Torr	At room temperature	N(E <sub>F</sub> ) cm <sup>-3</sup>	E <sub>g</sub> (ev <sup>-1</sup> )	Evaporation rate = thickness/time Angstrom/sec	Remarks
1.	a-Ge-H(1)	1.5x10 <sup>-4</sup> of H <sub>2</sub>	-	-	-	$\frac{2946}{60} = 49.1$	1. Non-ohmic 2. Very fast evapo- ration rate 3. without purifier
2.	a-Ge-H(2)	1.1x10 <sup>-4</sup>	-	-	-	$\frac{1692}{14x60} = 2.015$	1. Not perfectly ohmic 2. Without purifier
3.	a-Ge-H(3)	5x10 <sup>-5</sup>	4.5x10 <sup>-6</sup>	-	7.2x10 <sup>16</sup> ev	$\frac{2245}{15x60} = 2.49$	1. Ohmic 2. Without purifier H <sub>2</sub>
4.	a-Ge-H(4)	5x10 <sup>-5</sup>	2.23x10 <sup>-7</sup>	-	1.5x10 <sup>16</sup> ev	$\frac{400}{15x60} = 0.44$	1. Ohmic with purifier 2. Very low evaporation rate.
5.	a-Ge-H(5)	5x10 <sup>-5</sup>	7.2x10 <sup>-4</sup>	-	3.0x10 <sup>17</sup> ev(at 300°K)	$\frac{0.262}{20x60} \frac{1.875}{300°K} = 1.56$	1. Ohmic with purifier 2. Higher substrate temp. 340 K
6.	a-Ge-H(9)	1x10 <sup>-4</sup>	2.6x10 <sup>-3</sup>	-	5.5x10 <sup>17</sup> ev	$\frac{1.926}{15x60} = 2.140$	1. Ohmic with purifier 2. Substrate at higher temp. 340 K.

TABLE 3

Conductivity data of a-Ge and a-Ge-H for different partial pressures

(A) Substrate at Room Temperature (300 °K)

Sample	Pressure of H <sub>2</sub> Torr	$\sigma_{RT}$ ohm <sup>-1</sup> cm <sup>-1</sup>
a-Ge (1)	0	$1.68 \times 10^{-2}$
a-Ge-H (3)	$5 \times 10^{-5}$	$4.5 \times 10^{-6}$

(B) Substrate at high temperature (340 °K)

Sample	Pressure of H <sub>2</sub> Torr	$\sigma_{RT}$ ohm <sup>-1</sup> cm <sup>-1</sup>
a-Ge (4)	0	$3.25 \times 10^{-3}$
a-Ge-H (5)	$5 \times 10^{-5}$	$7.2 \times 10^{-4}$
a-Ge-H (9)	$1 \times 10^{-4}$	$2.76 \times 10^{-3}$

TABLE 4

Density of States of a-Ge-H for different Partial Pressure of Hydrogen

Sample	Pressure of $H_2$ Torr	To	$N(E_f) \text{ cm}^{-3} \text{ ev}^{-1}$
a-Ge (4)	0	$8.48 \times 10^7$	$2.19 \times 10^{18}$
a-Ge-H (5)	$5 \times 10^{-5}$	$6.19 \times 10^8$	$3.0 \times 10^{17}$
a-Ge-H (9)	$1 \times 10^{-4}$	$5.27 \times 10^8$	$3.5 \times 10^{17}$

TABLE 5

Activation energy of a-Ge-H for different partial pressures of hydrogen

Sample	$P_H$ (torr)	$E_f$ (ev)	Remark
a-Ge (4)	0	0.12	
a-Ge-H (5)	$5 \times 10^{-5}$	0.26	From low temperature measurements
a-Ge-H (9)	$1 \times 10^{-4}$	0.19	

TABLE 6

Effect of annealing on a-Ge-H films

Sample	Pressure of Hydrogen Torr	$\sigma_{RT} \text{ ohm}^{-1} \text{cm}^{-1}$	$\sigma_{RT}$ after annealing
a-Ge (2)	0	$6.9 \times 10^{-3}$	$3.01 \times 10^{-3}$ (at $390^{\circ}\text{K}$ )
			$1.36 \times 10^{-3}$ (at $420^{\circ}\text{K}$ )
a-Ge-(4)	0	$3.29 \times 10^{-3}$	$1.55 \times 10^{-3}$ ( $381.5^{\circ}\text{K}$ )
a-Ge-H (5)	$5 \times 10^{-5}$	$6.7 \times 10^{-4}$	$4.8 \times 10^{-4}$ ( $374^{\circ}\text{K}$ )
a-Ge-H (9)	$1 \times 10^{-4}$	$2.46 \times 10^{-3}$	$1.78 \times 10^{-3}$ ( $375^{\circ}\text{K}$ )

TABLE 7

Conductivity of a-Ge for different substrate temperature

Sample	Substrate Temperature	Pressure Torr	$\sigma_{RT} \text{ ohm}^{-1} \text{cm}^{-1}$
a-Ge (1)	Room Temperature 300°K	$5 \times 10^{-6}$	$1.68 \times 10^{-2}$
a-Ge (4)	340 °K	$5 \times 10^{-6}$	$3.3 \times 10^{-3}$

TABLE 8

Conductivity of a-Ge-H for different rate of deposition

Sample	Pressure of H <sub>2</sub> Torr	Rate of deposition A/sec	$\sigma_{RT} \text{ ohm}^{-1} \text{cm}^{-1}$
Ge-H (4)	$5 \times 10^{-5}$	$\frac{400}{15 \times 60} = 0.444$	$2.23 \times 10^{-7}$
Ge-H (5)	$5 \times 10^{-5}$	$\frac{1875}{20 \times 60} = 1.562$	$7.22 \times 10^{-4}$

REFERENCES

1. AIP Conference Proceedings No. 20 - Tetrahedrally Bonded Amorphous Semiconductors, H.H. Brodsky, S. Kirkpatrick, D. Weaire.
2. W.E. Spear and P.G. Le Comber, Solid State Commun. Vol. 17, 1193 (1975); Phil. Mag. Vol. 33, 935 (1976).
3. T.M. Donovan and K. Heinmann, Phys. Rev. Lett. 27, 1794 (1971).
4. F.L. Galeener, Phys. Rev. Lett. 27, 421 (1971).
5. R.J. Temkin, W. Paul, G.A.N. Connell, Adv. in Phys., 22, 58 (1973).
6. N.J. Shevchik and W. Paul, Journal of Non-crystalline Solids, 16, 55 (1977).
7. S.C. Mors and J.R. Gracyzk, Phys. Rev. Lett., 23, 1167 (1967).
8. G.S. Cargil, Phys. Rev. Letts. 1372 (1972).
9. M.H. Brodsky, R.S. Title, Phys. Rev. Letts. 23, 581 (1969).
10. N.F. Mott and E.A. Davis, Electronic Processes in Non-crystalline Solids, Clarendon Press, Oxford (1971).
11. M.M. Brodsky, K. Weiser, G.D. Pettit, Phys. Rev. B-1 2632 (1970).
12. A.J. Lewis, Phys. Rev. B-13, 2565 (1976).
13. A.J. Lewis, G.A.N. Connell, W. Paul, J.R. Pawlik, and R.J. Temkin, AIP Conference Proceeding No. 20.

14. M.H. Brodsky and R.J. Gambino - J. Non-cryst. Solids 8-10, 739 (1972).
15. S.C. Agarwal, Phys. Rev. B-7, 685 (1973).
16. P.G. Lecomber, W.E. Spear, D.J. Jones, Journal of Non-Cryst. Solids. 20, 259 (1976).
17. J.J. Hauser - PG Solid State Communication, 19, 1049 (1976).
18. G.A.N. Connell, J.R. Pawlik, J.R., Phys. Rev. B13, 787 (1976).
19. A.J. Lewis, Phys. Rev. B14, 658 (1976).
20. H. Fritzsche, C.G. Tsai, P. Pearson, Solid St. Tech., 55 (1978).
21. L. Maissel and P. Glang. Handbook of Thin Film Technology, McGraw Hill, N.Y. (1970).
22. M. Kastner and H. Fritzsche - Material Research Bulletin, 5th Volume, 631 Page, 1970.
23. V. Kumar, M.Tech. Thesis, I.I.T. Kanpur (1980).
24. N.F. Mott, Phil. Mag. 19, 835 (1969).
25. M.H. Brodsky and R.J. Gambino, Journal of Non-Crystalline Solids B-10, 739 (1972).
26. P.K. Wally, Thin Solid Films, 2, 327 (1968).
27. S.C. Agarwal, S. Guha and K.L. Narsimhan, Journal of Non-Cryst. Solids 18, 429 (1975).
28. K. Yasuda and T. Arizumi, Phys. Stat. Solidi 41, 181 (1977).
29. M. Fritzsche, C.C. Tsai and P. Persans, Solid St. Tech. 85 (1978).
30. S. Hasegawa and M. Kitagawa, Solid St. Comm. 27, 855 (1978).
31. D.K. Paul and S.S. Mitra, Phys. Rev. Letters, 31, 1000 (1975).